

RSC Advances



This is an *Accepted Manuscript*, which has been through the Royal Society of Chemistry peer review process and has been accepted for publication.

Accepted Manuscripts are published online shortly after acceptance, before technical editing, formatting and proof reading. Using this free service, authors can make their results available to the community, in citable form, before we publish the edited article. This *Accepted Manuscript* will be replaced by the edited, formatted and paginated article as soon as this is available.

You can find more information about *Accepted Manuscripts* in the [Information for Authors](#).

Please note that technical editing may introduce minor changes to the text and/or graphics, which may alter content. The journal's standard [Terms & Conditions](#) and the [Ethical guidelines](#) still apply. In no event shall the Royal Society of Chemistry be held responsible for any errors or omissions in this *Accepted Manuscript* or any consequences arising from the use of any information it contains.



Theoretical Study on the BINOL-Zinc Complex-Catalyzed Asymmetric Inverse-Electron-Demand Imino Diels-Alder Reaction: Mechanism and Stereochemistry

Received 00th January 20xx,
Accepted 00th January 20xx

DOI: 10.1039/x0xx00000x

www.rsc.org/

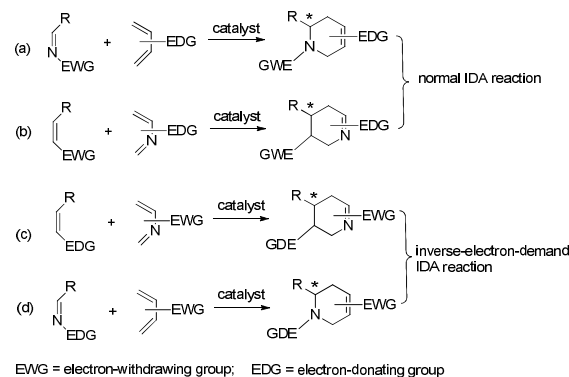
Weiyl Li,^{*a} Na Yang,^b and Yajing Lv^a

The mechanism and stereochemistry of an inverse electron-demand imino Diels-Alder (IEDIDA) reaction between a cyclic imine and an electron-poor chromone-derived diene catalyzed by a chiral BINOL-Zinc complex has been studied using a combination of DFT calculations, chemical reactivity indices and distortion/interaction analyses. The calculations reveal that the coordination of Lewis acid zinc catalyst to the ester C=O group of the electrophilic diene significantly lowers the energy barriers of the cycloaddition reaction by an increase of the electrophilic character of the diene. Herein, both catalytic mechanism and stereochemistry of the cycloadduct depend on the configuration of the diene. An energy-favored stepwise mechanism is adopted when the ester C=O group of the diene takes the *trans* configuration. This configuration allows a stabilizing interaction formed between the zinc center of the catalyst and the phenyl moiety of the dienophile and favors the steric discrimination from the naphthalene ring of the BINOL ligand at the ring-closure transition state that is rate-determining and stereo-controlling for the entire cycloaddition process. The electrophilic/nucleophilic interaction defines the most favored alignment between the dienophile and the diene-catalyst complex, which overwhelms the distortion of these fragments and realizes the *exo*-selectivity of the cycloadduct.

1. Introduction

The imino Diels-Alder reaction (IDA),¹ initiated by the dienophile (as an imine derivative) or by the diene (as a 1- or 2-azadiene), is a powerful synthetic route for the construction of various chiral nitrogen-containing six-membered heterocycles, such as piperidines, tetrahydroquinolines, quinolines and so on (Scheme 1). The resultant aza-heterocycles and their derivatives can be widely used as starting materials or intermediates in the total synthesis of many natural products and complex biologically active molecules.² Consequently, much effort has been devoted to the development of the asymmetric IDA reaction in order to obtain chiral aza-heterocycles with high yields and enantioselectivities.

Experimentally, a number of the normal IDA reactions between the electron-poor or electron-neutral imines and the electron-rich dienes have been realized. For example, a series of chiral Lewis acids catalysts combined with the BINOL ligands and a variety of metals (Zr^{3a-e}, Nb^{3f-i}, and Zn^{3j-k}) were found to be effective in the catalytic asymmetric IDA reactions of



Scheme 1 Strategies for synthesis of aza-heterocycles via the imino Diels-Alder reactions.

electron-poor imines with Danishefsky's diene. The metal center of the catalyst serves as a Lewis acid to activate the nitrogen center of the imine and increase the electrophilicity of the dienophile. The 3,3'-positions of the BINOL ring provides the asymmetric environment for the enantioselective cycloaddition of dienes. Shortly after these reports were published, a variety of chiral Lewis catalytic systems like BINAP-Cu,^{4a-b} N,P-oligopeptide-Ag,^{4c} VAPOL-boron,^{4d} and *N,N'*- α -dioxide-metals^{4e-i} were developed for the IDA reaction between dienophile imines and Danishefsky's diene, which aimed at increasing the enantioselectivities of cycloadducts, decreasing of catalysts loading and expanding the scope of the substrates. In addition, as one kind of useful and powerful

^aSchool of Science, Xihua University, Chengdu, 610039, Sichuan, P. R. China.

† E-mail address: weiyili@mail.xhu.edu.cn

^bInstitute of Nuclear Physics and Chemistry, China Academy of Engineering Physics, Mianyang, 621900, P. R. China

Tel: +86-028-87727663; Fax: +86-028-87727663;

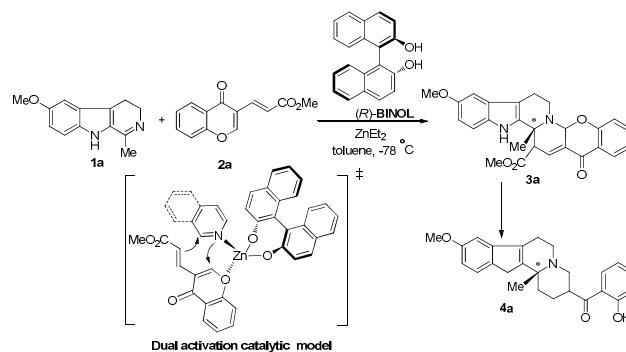
Electronic Supplementary Information (ESI) available: Computational details, optimized geometries, calculated energies and the full citation of Gaussian 09 program. See DOI: 10.1039/x0xx00000x

catalysts, many environmental-friendly bifunctional organocatalysts were also successfully applied to enhance the enantioselective IDA reactions of imino-dienophiles with dienes. Ohsawa and co-workers^{5a} reported the first example of L-proline-catalyzed IDA reaction of cyclic imines and methyl vinyl ketones, which leads to the production of the precursors of natural indole alkaloids with good yields and excellent enantioselectivities. They also proposed the final cycloadduct was obtained via an enamine active intermediate generated from enone and proline in the Mannich-type fashion.^{5b} Afterward, the modification of the amino acid scaffold on the proline catalyst was performed in order to increase the solubility of the catalyst and expand the scope of the reaction. Differing from the proline-catalyzed IDA reaction, the activation of the dienophile imines by chiral Brønsted phosphoric acids occurs primarily via hydrogen-bonding interactions. Akiyama et al.⁶ discovered that BINOL-derived phosphoric acids prove as efficient catalysts for the IDA reaction of imines with both Danishefsky's diene and Brassard's diene. The IDA reaction of an imine with the non-activated diene cyclohexenone was also achieved using a cooperative catalyst combined with the chiral phosphoric acid and acetic acid, in which acetic acid played the essential role in accelerating the reaction rate.⁷

In addition to the normal IDA reaction, the asymmetric inverse electron-demand imino Diels-Alder (IEDIDA) reaction between the electron-deficient 2-aza-butadiene and an electron-rich dienophile was also investigated in the presence of chiral Lewis acids⁸ and organocatalysts.⁹ The catalytic methodologies can be classified into three categories: (i) activation of the diene by Lewis acidic metal complexes or organocatalysts; (ii) activation of dienophiles via the generation of an enamine or enolate intermediate; and (iii) the dual activation strategy of both the dienophiles and of dienes. To the best of our knowledge, azadienes were employed as electron-deficient component in the almost reported cases.¹⁰ Examples of IEDIDA reaction between electron-rich imines and electron-deficient dienes are rather rare.

Very recently, Kumar and Waldmann reported the first case of an asymmetric IEDIDA reaction that is the cycloaddition of the electron-rich cyclic imine **1a** with the chromone-derived diene **2a** in the presence of the Lewis acid zinc and (*R*)-BINOL ligand (Scheme 2).¹¹ The target indoloquinolizine **4a** was obtained through the intermediary cycloadduct **3a** with moderate yield (51%) and high an enantiomeric excess (ee) value (93%). The authors also suggested a dual activation catalytic model to explain the observed enantioselectivity. In this model, both the nitrogen atom of the imine moiety and the oxygen atom of the vinylogous ester diene are coordinated with the zinc center. However, this model seems not to fit within the three catalytic categories as mentioned previously, because the coordination of the nitrogen atom of the imine moiety with the Lewis acid center might decrease the electron density of the dienophile and disfavor the cycloaddition with an electron-deficient diene. Furthermore, the detailed reaction mechanism, the origin of the regioselectivity, the *endo/exo* selectivity and the enantioselectivity of the reaction are altogether unclear.

Herein, we carried out a comprehensive theoretical investigation on the titled reaction to further understand the mechanism and the stereochemistry of this novel reaction at the molecular level. The catalytic role and the chiral introduction of the BINOL-Zn complex were examined by a combination of DFT calculations, reactivity indices and distortion/interaction analyses, which are expected to provide useful information for the design of more and efficient asymmetric IEDIDA reactions.



Scheme 2 Asymmetric IEDIDA reaction between the imine dienophile **1a** and chromone-derived diene **2a** in the presence of Lewis acid zinc and (*R*)-BINOL ligand.

2. Computational methods

Among the correlated density functional methods, the hybrid *meta* exchange-correlation M05-2X, developed by Zhao and Truhlar, performs well in main group thermochemistry, kinetics, and noncovalent interactions.¹² Particularly, the M05-2X method also gives accurate geometry optimization and energetic calculations for zinc compounds, which has been demonstrated in previous theoretical investigations.¹³ Accordingly, the geometry optimization of all reactants, products, intermediates (IMs) and transition states (TSs) involved in the present system was carried out using the M05-2X functional with the 6-31G(d) basis set.¹⁴ The vibrational frequencies were calculated at the same level to characterize each optimized structure is an intermediate (no imaginary frequency) or a transition state (unique imaginary frequency) and obtain the thermal corrections at 298 K. Intrinsic reaction coordinates (IRC)¹⁵ scans were conducted when necessary to ensure the transition state correctly connects the two relevant minima. To consider the solvent effect, single-point energy calculation in toluene (experimentally used) was performed on the gas-optimized structure with the SMD¹⁶ continuum solvation model at the M05-2X/6-311+G(d,p) level. Unless otherwise specified, the relative free energies (ΔG) including the thermal corrections in the gas phase and the single-point energies in the solvent were reported.

In addition, exhaustive theoretical studies on a series of DA reactions by Domingo et al.¹⁷ shown that the reactivity indices defined within the conceptual DFT framework were very useful tools to understand the reaction mechanism and explain the chem- and regioselectivity in the polar cycloaddition reactions.

Accordingly, the electronic chemical potential μ , chemical hardness η , and the global electrophilicity ω and nucleophilicity N were calculated, respectively, at the ground state (GS) of the molecules.^{18,19} The local reactivity electrophilicity ω_k and nucleophilicity indices N_k for the reactants and molecular complex were also calculated based on the Parr function, recently proposed by Domingo,²⁰ using the following equations,

$$\omega_k = \omega P_k^+ \quad (1)$$

$$N_k = NP_k^- \quad (2)$$

Where P_k^+ is the electrophilic Parr functions obtained from atomic spin density (ASD) analysis at the radical anion, and P_k^- is the nucleophilic Parr functions obtained from ASD analysis at the radical cation.

The global electron density transfer (GEDT)²¹ is a global flux of electron density taking place from the nucleophile to the electrophile, which could be one of the key factors in determining the activation energy. This value at the TS was computed by sharing the nature charge through natural bond orbital (NBO)²² analysis between the nucleophilic and the electrophilic frameworks.

To gain an insight into the origin of the *endo/exo* selectivity in the reaction, distortion/interaction analysis,²³ recommended by Houk and co-workers in cycloaddition reactions, was carried out on the corresponding the TSs. By definition, the activation energy (ΔE^\ddagger) is decomposed into the distortion energy ($\Delta E_{\text{dist}}^\ddagger$) and the interaction energy ($\Delta E_{\text{int}}^\ddagger$), $\Delta E^\ddagger = \Delta E_{\text{dist}}^\ddagger + \Delta E_{\text{int}}^\ddagger$. The $\Delta E_{\text{dist}}^\ddagger$ is the energy required to distort the reactants and catalysts into the geometry they have in the transition states and $\Delta E_{\text{int}}^\ddagger$ is a negative value which indicates favorable interaction between the reactants and catalysts.

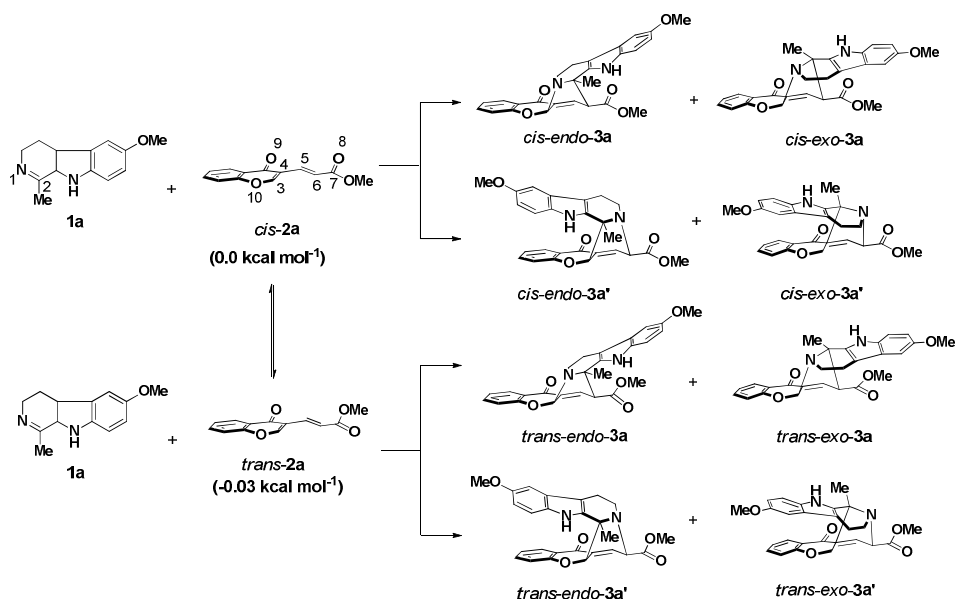
All DFT calculations were carried out with the Gaussian 09 software package.²⁴ The three-dimensional molecular structures were drawn using the CYLVIEW program²⁵.

3. Results and Discussion

3.1 Background reaction without catalyst

For the chromone-derived diene **2a**, the C7=O8 double bond of the ester group might adopt a *cis* or *trans* configuration relative to the C5=C6 double bond (Scheme 3). In this work, the cycloaddition of imine dienophile **1a** with both *cis*- and *trans*-**2a** was simulated because the free energy difference between these two isomers is less than 0.1 kcal mol⁻¹. Moreover, the reaction mechanism and the stereochemical outcome of this reaction were also found to be very sensitive to the configuration of the diene (*vide infra*). Hence, four possible reaction channels (*cis-endo*, *cis-exo*, *trans-endo*, and *trans-exo*) are in principle available in the background reaction, resulting in eight different products: *cis* or *trans* isomer for each of the two regio-isomers (**3a** and **3a'**), and an *endo* and *exo* approach for each of the two regio-isomers. To make a concise expression, *trans* reaction channels will be discussed with emphasis in what follows. The details along *cis* reaction channels are provided in the ESI (Section S2.1).

Initially, the reactivity indices of the reactants were analyzed (Table 1). The electronic chemical potential of imine **1a** ($\mu = -3.7$ eV) is found to be higher than that of *trans*-**2a** ($\mu = -4.8$ eV). Indeed, **1a** with high global nucleophilicity index ($N = 4.0$ eV) and low global electrophilicity index ($\omega = 1.0$ eV) can be classified as a strong nucleophile ($N > 3.0$).²⁶ For diene *trans*-**2a**, the global nucleophilicity index ($N = 2.8$ eV) is also larger than its electrophilicity index ($\omega = 1.6$ eV). However, *trans*-**2a** can only serve as the electrophile in this cycloaddition reaction. Consequently, the GEDT will flux from the nucleophile **1a** to the electrophile *trans*-**2a** during the cycloaddition process. These results confirm that this [4+2] cycloaddition reaction requires inverse-electron-demand. Additionally, the computed Parr Fukui functions based on the atomic spin density suggest a higher nucleophilic site at the N1 position of the imine group,



Scheme 3. Possible reaction channels for the uncatalyzed IEDIDA reaction between **1a** and **2a**.

Table 1 Electronic chemical potential μ , chemical hardness η , global electrophilicity ω , global nucleophilicity N , electrophilic Parr function P_k^+ , local electrophilicity ω_k , electrophilic Parr function P_k^- and local nucleophilicity N_k indices for **1a**, *trans-2a* and catalyst-reactants molecular complexes.

Species	μ [eV]	η [eV]	ω [eV]	N [eV]	P_k^+ (Mulliken)		ω_k [eV]		P_k^- (Mulliken)		N_k [eV]	
					C3	C6	C3	C6	N1	C2	N1	C2
1a	-3.7	6.6	1.0	4.0	-	-	-	-	0.27	0.13	1.1	0.5
COM-I	-4.7	6.8	1.6	3.0	-	-	-	-	0.27	0.03	1.0	0.3
COM-II	-4.8	6.1	1.7	3.2	-	-	-	-	0.21	0.36	0.7	1.2
<i>trans-2a</i>	-4.8	7.0	1.6	2.8	0.57	0.10	0.9	0.2	-	-	-	-
<i>trans-COM-III</i>	-5.5	7.1	2.1	2.1	0.50	0.06	1.1	0.1	-	-	-	-
<i>trans-COM-IV</i>	-5.7	6.7	2.5	2.0	0.42	-0.02	1.1	0.0	-	-	-	-
<i>trans-COM-V</i>	-5.7	6.4	2.5	2.1	0.47	0.20	1.2	0.5	-	-	-	-
<i>trans-COM-VI</i>	-5.4	6.8	2.1	2.3	0.36	0.15	0.8	0.3	-	-	-	-
<i>trans-COM-VII</i>	-5.5	6.6	2.3	2.2	0.43	0.07	1.0	0.2	-	-	-	-

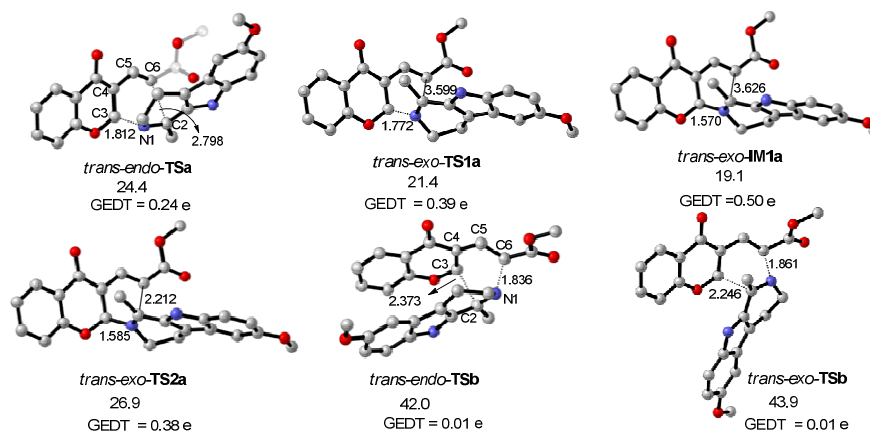


Figure 1. The M05-2X/6-31G(d)-optimized TSs and IMs structures for the uncatalyzed IEDIDA reaction of **1a** and *trans-2a* (the bond distances are labeled in Å and the Gibbs free energies relative to separate reactants are given in kcal mol⁻¹).

$P_k^- = 0.27$, than the C2 atom with $P_k^- = 0.13$. In *trans-2a*, the conjugated C3 position is predicted to be more electrophilic than the C6 position, as verified by the higher Parr Fukui functions electrophilic P_k^+ (0.57 for the C3 atom *a* 0.10 for the C6 atom). As a consequence of the activity differences between the reaction sites, the relative free energies of TSs *trans-endo-TS1a*, *trans-exo-TS1a* and *trans-exo-TS2a*, corresponding to the construction of N1–C3 and C2–C6 bonds, are less energetic than TSs *trans-endo-TSb* and *trans-exo-TSb*, leading to the formation of N1–C6 and C2–C3 bonds (Figure 1). Therefore, there is a pronounced regioselectivity for this cycloaddition reaction, yielding the cycloadduct *trans-endo-3a* or *trans-exo-3a* as the major product. The calculations well reproduced the experimental observations that *trans-endo-3a'* and *trans-exo-3a'* were not yielded in this cycloaddition reaction.¹¹ Along the more favourable region-isomeric reaction channel, the *trans-endo* stereoisomer is generated via a one-step two-stage mechanism. At TS *trans-endo-TS1a*, the length of the N1–C3 forming bond (1.812 Å) is shorter than that of the C2–C6 forming bond (2.798 Å). This large difference ($\Delta d = 0.986$

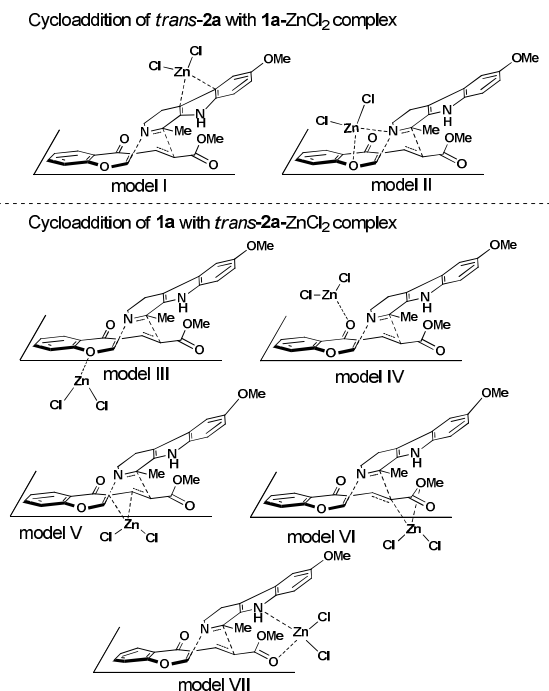
Å) between the lengths of the two forming bonds suggests that TS *trans-endo-TS1a* correspond with concerted but highly asynchronous bond-formation process where the N1–C3 forming bond is being formed in a larger extension than the C2–C6 one. The GEDT from the nucleophilic **1a** to the electron-deficient *trans-2a* at TS *trans-endo-TS1a* is 0.24 e, indicating this cycloaddition process belongs to a polar DA reaction ($0.15 \text{ e} < \text{GEDT} < 0.40 \text{ e}$).^{17f} The comparison of the GEDT values with the unfavorable TSs *trans-endo-TSb* and *trans-exo-TSb* (0.01 e) suggests that the GEDT is the main factor controlling the reaction rate of the DA reactions.^{17f} With respect to separate reactants, the activation energy (ΔE^\ddagger), activation enthalpy (ΔH^\ddagger) and activation free energy (ΔG^\ddagger) barrier for TS *trans-endo-TS1a* is 8.4, 7.6, and 24.4 kcal mol⁻¹, repetitively (Table S2). These results can well account for the reaction temperature (80 °C) required for the uncatalyzed reaction.¹¹ Alternatively, calculations show that the *trans-exo* cycloadduct is yielded through a stepwise mechanism, with the forming a zwitterionic intermediate *trans-exo-IM1a*. This result is different with the *trans-endo* channel as well as the *cis-exo*

channel when diene *cis*-**2a** is employed (Figure S1 in ESI). The geometric optimizations in toluene using SMD solvation model also gave the same result, indicating that the inclusion of solvent effect does not alter the reaction mechanism. Based on the analysis of molecular orbitals (Figure S2~3 in ESI), this discrepancy might be attributed to the fact that the phase of the π orbital of the pyrrole and phenyl moieties in the HOMO of **1a** cannot match with that of the p orbital of the ester carbonyl oxygen atom in the LUMO of *trans*-**2a**. Consequently, the N1–C3 bond formation is initially formed via TS *trans*-*exo*-**TS1a**, in which the length of the forming N1–C3 is 1.772 Å, whereas the bond distance between C2 and C6 atom is still long as 3.599 Å. This long bond distance suggests that there is no interaction between C2 and C6 centers during the N1–C3 bond formation. Compared with TS *trans*-*endo*-**TSa**, TS *trans*-*exo*-**TS1a** is predicted with a larger polarity, as reflected by the larger GEDT value of 0.39 e. Thus, the relative free energy of TS *trans*-*exo*-**TS1a** is calculated to be 3.0 kcal mol⁻¹ lower than that of *trans*-*endo*-**TSa**. After TS *trans*-*exo*-**TS1a**, the N1–C3 bond is formed in IM *trans*-*exo*-**IM1a**, and the GEDT value of IM *trans*-*exo*-**IM1a** is increased to 0.50 e. This high value indicates that IM *trans*-*exo*-**IM1a** has zwitterionic characteristics (GEDT > 4.0 e). Finally, the *trans*-*exo* cycloadduct can be generated via a ring-closure TS *trans*-*exo*-**TS2a**, which requires a higher energy barrier of 26.9 kcal mol⁻¹. The GEDT value at TS *trans*-*exo*-**TS2a** is 0.38 e, which is similar that of TS *trans*-*exo*-**TS1a** (0.39 e). Hence, the increased energy barrier at the ring-closure step might be caused by the electrostatic repulsion between the pyrrole and phenyl moieties of **1a** and the ester carbonyl group of *trans*-**2a** when C2 and C6 centers approach one another at TS *trans*-*exo*-**TS2a**. Additionally, since this cycloaddition process presents a stepwise mechanism, the diradical structures could in principle be involved. The stability of wave functions for the TSs and IMs involved was tested with the unrestricted UM05-2X method. The UM05-2X/6-31G* calculations predict that wave functions are stable and the optimized-structures are the same as the corresponding ones obtained from the restricted M05-2X/6-31G*. The triplet structures exist but lies about 10.0~15.0 kcal mol⁻¹ above the singlet ones in free energy. Therefore, diradical mechanism can be ruled out for the *trans*-*exo* channel. Overall, for the background reaction between **1a** and *trans*-**2a**, the *endo* selectivity is kinetically preferred to the *exo* selectivity by 2.5 kcal mol⁻¹ in kinetics. The reaction Gibbs free energies (ΔG_{rxn}) for generation of *trans*-*endo*-**3a** and *trans*-*exo*-**3a** are endothermic by 8.4 and 5.6 kcal mol⁻¹, respectively. Thus, these intermediary cycloadducts will spontaneously convert to indoloquinolizine *trans*-*endo*-**4a** and *trans*-*exo*-**4a** with the release of 14.0 and 13.0 kcal mol⁻¹ in free energy, respectively.

3.2 Catalytic reaction mechanism

Kumar's experiment showed that either the reaction temperature could be lowered or the reaction time could be shortened when Lewis acid catalyst zinc catalyst was added into the reaction system.¹¹ To shed light on the actual catalytic

role of this Lewis acid catalyst, the mechanistic investigation on the IEDIDA reaction of **1a** with both *cis* and *trans*-**2a** in the presence of the simple ZnCl₂ were carried out in this section. Seven modes of activation, depending on where ZnCl₂ coordinates to the two substrates are considered (Scheme 4).



Scheme 4. Proposed reaction models for the ZnCl₂-catalyzed IEDIDA reaction between **1a** and *trans*-**2a**.

Cycloaddition of *trans*-**2a** with **1a**-ZnCl₂ complexes

Initially, the geometries at the energy minima of the two kinds of molecular complexes (**COM-I** and **COM-II**) formed between **1a** and ZnCl₂ were found, differing in the coordination mode of **1a** with the zinc center of Lewis acid (Figure 2). When the C=C double bond in the pyrrole ring of **1a** is η^2 -bonded to the zinc center, complex **COM-I** is formed, lying 5.7 kcal mol⁻¹ below the two individual species in free energy. As compared with free **1a**, the chemical potential μ is decreased to -4.7 eV, while the global electrophilicity index ω for complex **COM-I** is increased to 1.6 eV. Thus, the electrophilicity difference ($\Delta\omega$) between complex **COM-I** and *trans*-**2a** is decreased to zero, indicating a very lower polar character for the cycloaddition of complex **COM-I** with *trans*-**2a**.^{17b} The calculations show that the cycloaddition of complex **COM-I** with *trans*-**2a** undergoes a one-step two-stage concerted mechanism for both *endo* and *exo* approaches. As expected, the GEDT values at TSs *trans*-*endo*-**TS-I** and *trans*-*exo*-**TS-I** are decreased to 0.14 e and 0.18 e, respectively, which are even lower than those in the background reaction. Meanwhile, differences between the lengths of the two forming bonds (Δd) at these two TSs are also decreased to 0.855 and 0.780 Å, respectively. These changes indicate that the polarity for these cycloaddition processes and asynchronicity at the two TSs are both lowered.

The relative free energies of *trans-endo-TS-I* and *trans-exo-TS-I* are reduced to 18.8 and 22.2 kcal mol⁻¹, respectively, with respect to the corresponding ones in the background reaction. However, the energy barriers for these two TSs measured from complex **COM-I** are comparable or even higher (24.5 and 28.9 kcal mol⁻¹, respectively). On the other hand, ZnCl₂ acting as a Lewis acid, extremely trends to combine with the basic center (N1 atom) of **1a**, which leads to the generation of a stable complex **COM-II** by exothermic of 23.8 kcal mol⁻¹ in free energy. This complexation also makes the decrease of the chemical potential μ ($\mu = -4.7$ eV) and the increase of the global electrophilicity for the complex **COM-II**, and therefore might disfavor the polarity for the cycloaddition process between complex **COM-II** and *trans-2a*. From complex **COM-II**, the cycloaddition reaction with *trans-2a* also takes place along a concerted but weakly asynchronous mechanism for both *endo* and *exo* channels, as suggested by the smaller difference between the lengths of the two forming bonds ($\Delta d = 0.576$ Å for *trans-endo-TS-II* and 0.309 for *trans-exo-TS-II*). At TS *trans-*

endo-TS-II, it can be noticed that the vinylogous ester oxygen (O7) atom in diene *trans-2a* is coordinated to the zinc center of the Lewis acid with a Zn–O bond distance of 2.240 Å, which corresponds to the dual activation model proposed by Kumar.¹¹ This interaction is slightly weaker in TS *trans-exo-TS-II*, as suggested by the longer Zn–O bond distance of 2.782 Å. With this stabilization, the relative free energy of the *endo* TS is 5.7 kcal mol⁻¹ more favorable than the *exo* one, although the GEDT value at TS *trans-exo-TS-II* is found to be 0.1 e larger than that at TS *trans-endo-TS-II*. Nevertheless, the free energy barrier for overcoming TS *trans-endo-TS-II* is increased to 43.5 kcal mol⁻¹, meaning that this dual activation catalytic model cannot be responsible for the catalytic role of ZnCl₂ in the reaction.¹¹ The coordination of the Lewis acid zinc catalyst to the nucleophilic **1a** increases the electrophilicity of **1a**-ZnCl₂ molecular complex and decreases the polarity for the cycloaddition reaction, and thereby disfavors for lowering the activation free energy.¹⁷

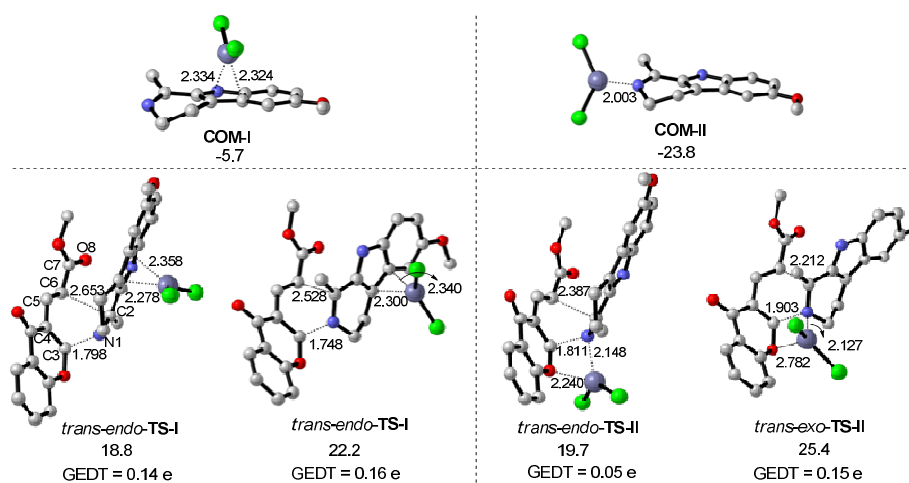


Figure 2. The M05-2X/6-31G(d)-optimized **1a**-ZnCl₂ complexes and TSs in the cycloaddition of **1a**-ZnCl₂ complexes with *trans-2a* (the bond distances are labeled in Å and the relative Gibbs free energies are given in kcal mol⁻¹).

Cycloaddition of **1a** with *trans-2a*-ZnCl₂ complexes

Subsequently, the catalysis reaction mechanism, that is the activation of the electrophilicity of *trans-2a* by the Lewis acid ZnCl₂, was investigated. As shown in Figure 3, five types of molecular complexes formed between diene *trans-2a* and ZnCl₂ were located as minima.

Among these five complexes, complexes *trans-COM-IV* and *trans-COM-VII*, formed by the coordination of the ester carbonyl oxygen atom (O8) and the ketone carbonyl oxygen atom (O9) of *trans-2a* to the zinc center, are predicted to be more stable in energy than the others, which lie 9.5 and 9.0 kcal mol⁻¹ below separate *trans-2a* and ZnCl₂, respectively. The presence of ZnCl₂ coordinated to the functional groups of *trans-2a* decrease the chemical potential μ of the *trans-2a*-ZnCl₂ molecular complexes, but increases their electrophilicity, as shown in Table 1. These changes enhances both chemical potential difference ($\Delta\mu$) and electrophilicity difference ($\Delta\omega$)

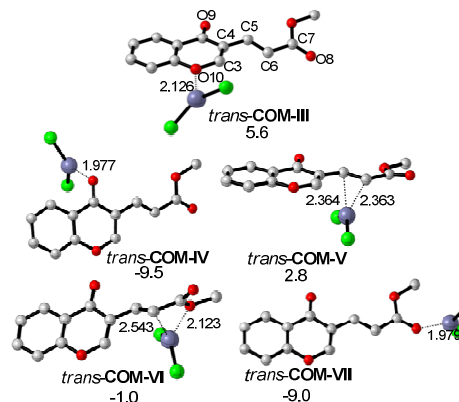


Figure 3. The M05-2X/6-31G(d)-optimized *trans-2a*-ZnCl₂ complexes (the bond distances are labeled in Å and relative Gibbs free energies are given in kcal mol⁻¹).

between **1a** and ZnCl_2 -*trans*-**2a** molecular complex, and will in consequence favors the charge transfer from nucleophilic **1a** to the electrophilic ZnCl_2 -*trans*-**2a** molecular complex and increase the polar character of the cycloaddition processes.¹⁷ The calculations show that the cycloaddition between the ZnCl_2 -*trans*-**2a** molecular complexes and **1a** nearly takes place along a stepwise process, except for the *trans-endo* model III from complex *trans*-COM-III (Figure S11 in ESI). The first step corresponds to the nucleophilic attack of the N1 atom of **1a** to the C3 atom of the ZnCl_2 -*trans*-**2a** complex to give acyclic zwitterionic intermediate. The second step corresponds to the ring-closure process at the zwitterionic intermediate with the production of the final [4+2] cycloadduct. The diradical mechanism was also ruled out by the unrestricted DFT calculations. The exhaustive exploration of the potential energy profiles for these five reaction channels (Figure S11~S14) allows us to determine the most energy-favorable reaction channel. As shown in Figure 4, the most energy-favorable reaction channel starts from complex *trans*-COM-VII, in which the ester C=O oxygen atom is bonded to the Lewis acid center. As this complex gets close to the imine moiety of **1a**, the intermolecular nucleophilic attack of the N1 atom of imine moiety on the C3 position initially occurs, leading to the formation of N1–C3 bond in IM *trans-endo*-IM1-VII or *trans-exo*-IM1-VII via TS *trans-endo*-TS1-VII or *trans-exo*-TS1-VII,

respectively. In TS *trans-endo*-TS1-VII, N1–C3 bond length of 1.841 Å is longer than in TS *trans-exo*-TS1-VII, while the distance between C2 and C6 (2.902 Å) is shorter than in TS *trans-exo*-TS1-VII (3.040 Å). At the same time, it can be noticed that the nitrogen atom of the pyrrole ring is strongly coordinated to the zinc center in the *endo* TS with the Zn–N bond distance of 2.307 Å, while a relatively weaker interaction (2.432 Å for Zn–C bond distance) between the carbon atom of phenyl ring and the zinc center is formed in the *exo* TS. As a result, the GEDT value at the *endo* TS *trans-endo*-TS1-VII (0.37 e) about 0.1 e smaller than in the *exo* one *trans-exo*-TS1-VII (0.48 e). The relative free energy of the *exo* TS is predicted to be 2.9 kcal mol⁻¹ preferred than that of the *endo* one. At TSs *trans-endo*-TS1-VII and *trans-exo*-TS1-VII, the N1–C3 Wiberg bond index (WBI) values are 0.48 and 0.56, respectively, while the C2–C6 WBI values are 0.02 and 0.02, respectively. At IMs *trans-endo*-IM1-VII and *trans-exo*-IM1-VII, the N1–C3 WBI values increase to 0.84 and 0.80, indicating these N1–C3 bonds are nearly formed, while the C2–C6 WBI values are remain to 0.04 and 0.02, respectively. The C6–C7WBI values at these IMs, 1.29 and 1.44, point out a certain π character for the C6–C7 bond as a result of the large delocalization of the negative charge on the C6 atom (–0.40 e in *trans-endo*-IM1-VII and –0.49 e in *trans-exo*-IM1-VII) belonging to the ester group. The interactions between the ester carbonyl oxygen atoms (O8)

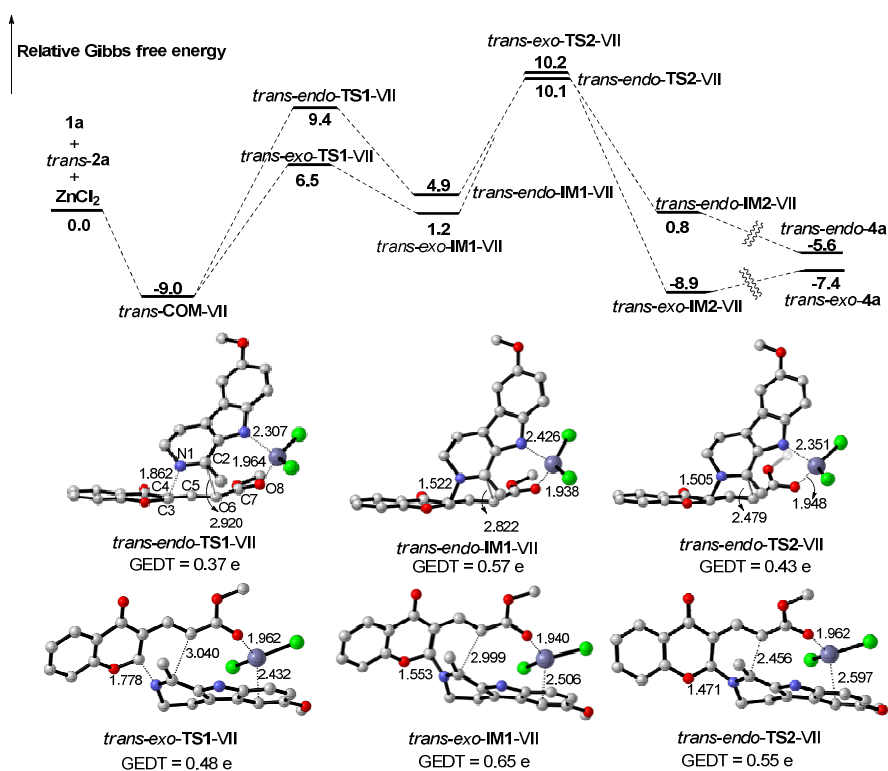


Figure 4. The energy profile (in kcal mol⁻¹) of the energy-favorable reaction channel for the ZnCl_2 -catalyzed IEDIDA reaction between **1a** and *trans*-**2a**, with the M05-2X/6-31G(d)-optimized TSs and IMs shown below (the forming bond distances are labeled in Å).

and the zinc center are also stronger, as verified by the shorter bond lengths of 1.938 and 1.940 Å. Thus, the accumulated negative charge on the C6 atoms can be dispersed and stabilized in these two zwitterionic IMs. Finally, the highly active zwitterionic **IM1s** can undergo an intramolecular nucleophilic addition of the electronegative C6 atom to the positive C2 atom via ring-closure **TS2s** *trans-endo-TS2-VII* and *trans-exo-TS2-VII*, respectively, allowing the production of [4+2] ring-formation products complexed with Lewis acid ZnCl₂. In the two ring-closure **TS2s**, the C2 and C6 atoms get closer with the bond distances of 2.479 and 2.456 Å, while the N1–C3 bond lengths are further shortened to 1.505 and 1.471 Å. The C2–C6 WBI values are 0.18 and 0.17, respectively, while the N1–C3 WBI values increase to 0.86 and 0.91, respectively. The GEDT values at the two ring-closure **TS2s** are 0.44 and 0.51 e, respectively, which are larger than those at the nucleophilic attack **TS1s** (0.37 and 0.48e) but smaller than those at the zwitterionic **IM1s** (0.43 and 0.57e). These trends show an increase of the GEDT along the nucleophilic attack of **1a** to the ZnCl₂-coordinated *trans-2a* up to formation of the zwitterionic **IM1s**, which is similar to the observation in the Lewis acid-catalyzed DA reaction.^{17a} However, the relative free energies of the ring-closure **TS2s** are predicted to 10.1 and 10.2 kcal mol⁻¹, which are higher than the nucleophilic attack **TS1s**. Thus, ring-closure step can be regarded as the rate-determining step (RDS) for the entire reaction, which is different with the calculations that RDS is the formation of zwitterionic IM in most of Lewis acid-catalyzed DA reactions.^{17a,27} In addition, although the GEDT value at *exo* TS for the ring-closure step is larger than that at the *endo* one, the relative free energies of these TSs are comparable. These observations cannot be explained by the differences of the GEDT values at the TSs. Consequently, the distortion/interaction analyses were performed on these four TSs in order to explore other factors that may influence the reaction activation barrier. The distortion energy $\Delta E_{\text{dist}}^{\ddagger}$ and the interaction energy ($\Delta E_{\text{int}}^{\ddagger}$) are summarized in Table 2. From the results of distortion/interaction analyses, it is clearly that the distortion energies $\Delta E_{\text{dist}}^{\ddagger}$ for the three fragments **1a**, *trans-2a* and ZnCl₂ decomposed from the two nucleophilic attack **TS1s** are comparable with one another. The total distortion energies ($\Delta E_{\text{dist}}^{\ddagger}$) of three fragments are identical. The preference for the *exo* TS in energy can be attributed to the favorable interaction energy $\Delta E_{\text{int}}^{\ddagger}$ (by 3.6 kcal mol⁻¹). This is in good accordance with the result of the higher GEDT value at the *exo* TS. For the ring-closure step, three fragments **1a**, *trans-2a*, and ZnCl₂ all suffer more heavily distortion at both *endo* and *exo* **TS2s**, than the corresponding ones at nucleophilic attack **TS1s**. Especially, for the diene moiety, the distorted energy is increased to 80.3 kcal mol⁻¹ at the *exo* TS, implying that high distortion energy is required for the diene moiety to achieve ring-closure TS overtake the favorable interaction. As a result, although the GEDT value at the *exo* TS is higher and the interaction energy $\Delta E_{\text{int}}^{\ddagger}$ is more favorable, the activation energy for the *exo* TS is similar to that for the *endo* one. The distortion energy should also be an important factor that controlled the reaction rate and the *endo/exo* selectivity.

Table 2 Activation energy ΔE^{\ddagger} , distortion energy $\Delta E_{\text{dist}}^{\ddagger}$ and interaction energies $\Delta E_{\text{int}}^{\ddagger}$ (all in kcal mol⁻¹) for the TSs involved along the most energy-favorable reaction channel.

Structures	$\Delta E_{\text{dist}}^{\ddagger a}$				$\Delta E_{\text{int}}^{\ddagger b}$	$\Delta E^{\ddagger c}$
	1a	<i>trans-2a</i>	ZnCl ₂	total		
<i>trans-endo-TS1-VII</i>	3.7	19.4	5.1	28.2	-42.1	-14.1
<i>trans-exo-TS1-VII</i>	2.6	21.3	4.3	28.2	-45.7	-17.5
<i>trans-endo-TS2-VII</i>	10.1	50.5	7.6	68.2	-83.1	-14.9
<i>trans-exo-TS2-VII</i>	9.5	80.3	6.2	96.0	-110.0	-15.0

^a $\Delta E_{\text{dist}}^{\ddagger}$ is the energy required to distort the reactants and catalysts into the geometry they have in the TSs;

^b $\Delta E_{\text{int}}^{\ddagger}$ is a negative value, indicating favourable interaction between the reactants and catalysts;

^c ΔE^{\ddagger} is the reaction activation energy.

Cycloaddition of **1a** with *cis-2a*-ZnCl₂ complex

On the other hand, we also investigated the mechanism of the IEDIDA reaction between **1a** with *cis-2a*-ZnCl₂ complexes. (S3.1 in ESI). Calculations indicate the most efficient channel remains the cycloaddition of **1a** with the complex *cis-COM-VII* in which ZnCl₂ is bonded with the ester carbonyl oxygen atom. When the ester C=O group adopts the *cis*-configuration relative to the C5=C6 double bond, the interaction of the zinc center to the dienophile and the catalytic mechanism slightly changes (Figure 5).

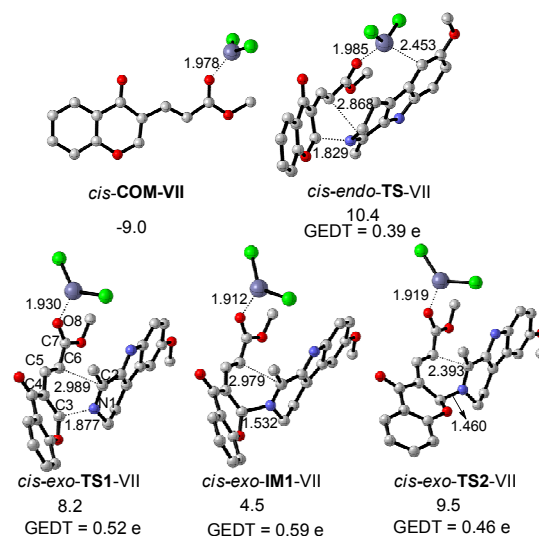


Figure 5. The M05-2X/6-31G(d)-optimized complex, IM and TSs involved in the cycloaddition of *cis-COM-VII* complex with **1a** (the bond distances are labeled in Å and the relative Gibbs free energies are given in kcal mol⁻¹).

Along the *endo* channel, the zinc center is simultaneously bonded with the ester carbonyl oxygen atom of *cis-2a* and the phenyl carbon atom of **1a**. The *cis-endo* cycloadduct is formed via a one-step two-stage concerted mechanism, without the generation of a zwitterionic IM. When the cycloaddition

reaction takes place along the *exo* approach, the zinc center is only bonded with ester carbonyl oxygen atom. The *cis-exo* cycloadduct is generated via a stepwise mechanism, and the ring-closure TS is also predicted to be RDS. The relative free energies of the RDS TSs (10.4 kcal mol⁻¹ for *cis-endo-TS-VII* and 9.5 kcal mol⁻¹ for *cis-exo-TS-VII*) along the *cis-endo* and *cis-exo* channels are similar to the corresponding ones along the *trans-endo* and *trans-exo* channels.

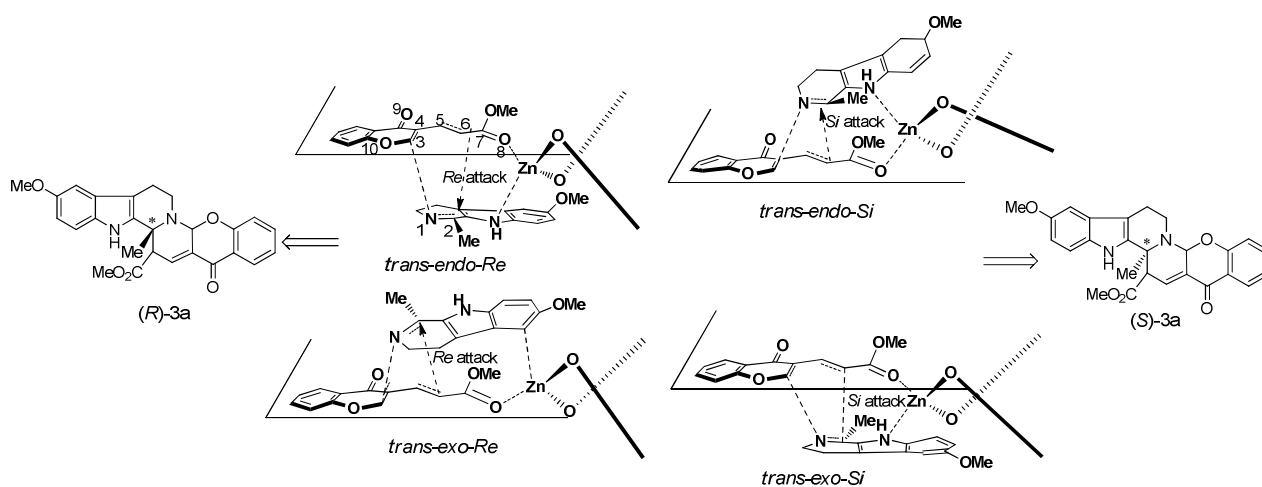
In summary, there is a notable decreasing of the activation energy in the Lewis acid ZnCl₂-catalyzed cycloaddition reaction relative to the uncatalyzed one. The reaction mechanism of nucleophilic **1a** with *trans*- or *cis*-COM-VII complex formed by the coordination of Lewis acid zinc to the ester C=O group of the *trans*- or *cis*-**2a** diene can be responsible for the experimental observation that reaction rate was accelerated as the Lewis acid catalyst was added.¹¹ The Lewis acid zinc catalyst plays a central role in increasing the electrophilicity the diene and stabilizing the zwitterionic intermediate by delocalizing the negative charge on the C6 atom of the diene.

3.3 The origin of stereochemistry

After understanding the mechanism of the cycloaddition of **1a** with **2a** catalyzed by simple Lewis acid ZnCl₂, our attention turns to the chiral BINOL-ligated-Zn complex-mediated reaction, because the origin of stereochemistry of the reaction is more attractive in asymmetric catalysis. Although an excellent enantioselectivity of 93% ee was achieved in the presence of the chiral (*R*)-BINOL ligand and the Lewis acid catalyst ZnEt₂,¹¹ the TS model assumed by Kumar and co-worker seems not be rationale to account for the origin of the stereochemical course of the reaction. In terms of the energetic comparison (Section S4.1 in ESI), the energy-favorable reaction channel is the addition of **1a** with BINOL-Zn-*trans*-**2a** complex in which the zinc center is coordinated to the ester carbonyl oxygen atom of the diene, which is the same as the outcome of the achiral system.

Starting from the complex formed between the BINOL-Zn catalyst and *trans*-**2a**, four possible reaction channels are located theoretically when the attack of the BINOL-Zn-*trans*-**2a** complex on the *Re* or *Si* face of the imine **1a** via the *endo* or *exo* approach is considered. These four channels are denoted as *trans-endo-Re*, *trans-endo-Si*, *trans-exo-Re*, and *trans-exo-Si* (Scheme 5). The optimized-structures and relative energies of the key TSs and IMs involved in the entire reaction are shown in Figure S17~19 in ESI. Calculations indicate that each of the reaction pathway proceeds through a stepwise mechanism with the formation of the zwitterionic intermediates. Along the PES of the four channels, the relative free energies of the ring-closure TSs are higher than those of TS1s. This trend is the same as the activation energy calculated in achiral system. Meanwhile, it is obviously that the chiral carbon atom (C6) in cycloadduct is generated in the ring-closure step. Therefore, the ring-closure step should be the stereo-controlling step for the entire reaction, and the enantioselectivity of the cycloadduct should depend on the relative energies of TS2s. The optimized-structures and the relative energies of TS2s are presented in Figure 6 and Table 3, respectively.

Of these four competing TSs, TSs *trans-endo-TS2-Re* and *trans-exo-TS2-Re*, corresponding to the *Re* face attack on the imine moiety of **1a**, are the lowest structures, which are favored over the other two structures by 1.1 and 3.1 kcal mol⁻¹ in free energy, respectively. Hence, the *R* configuration of the cycloadduct **3a** is predicted to be the major product, corresponding to the theoretically expected ee value of 99% using Boltzmann distribution of the four TSs at 298 K (Table 3). The computed result is qualitatively in agreement with the experimental observed outcome that the *R* configuration indoloquinoline was obtained with the enantioselectivity of 90% ee value. For the two energy-favorable TSs, the *exo* structure is 2.3 kcal mol⁻¹ preferred to the *endo* one, meaning that the *exo* cycloadduct should be the predominate product, which is different from the *endo* preference in the most of DA and HDA reactions.²⁸



Scheme 5. Proposed reaction models for the chiral BINOL-Zn-catalyzed the asymmetric IEDIDA reaction between **1a** and *trans*-**2a**.

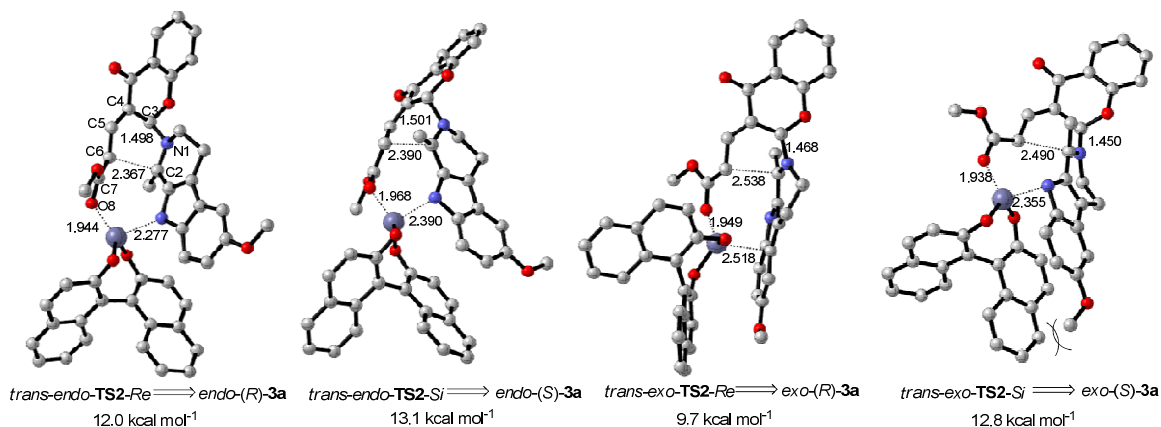


Figure 6. The M05-2X/6-31G(d)-optimized ring-closure TSs in the IEDIDA reaction between **1a** and *trans*-**2a** catalyzed by the chiral BINOL-Zn complex (the forming bond distances are labeled in Å and the relative free energies are given in kcal mol⁻¹).

Table 3 Activation energy, activation free energy, distortion and interaction energy, (all in kcal mol⁻¹) and GEDT value (in e) for the ring-closure TSs in the chiral BINOL-Zn-catalyzed IEDIDA reaction of **1a** with both *cis*- and *trans*-**2a**.

Species	$\Delta E_{\text{dist}}^{\ddagger}$				$\Delta E_{\text{int}}^{\ddagger}$	ΔE^{\ddagger}	ΔG^{\ddagger}	$\tau^{\ddagger}/\%$	GEDT
	1a	2a	catalyst	total					
<i>trans-endo-TS2-Re</i>	19.7	58.5	2.5	73.9	-98.9	-18.2	12.0	1.2	0.39
<i>trans-endo-TS2-Si</i>	18.5	56.7	2.6	77.8	-97.3	-19.5	13.1	0.2	0.42
<i>trans-exo-TS2-Re</i>	12.1	88.2	3.1	103.4	-123.8	-20.5	9.7	98.3	0.52
<i>trans-exo-TS2-Si</i>	15.6	93.2	2.8	111.7	-129.3	-17.6	12.8	0.3	0.50
<i>cis-endo-TS-Re</i>	6.4	25.4	2.4	34.2	-52.1	-18.0	12.4	37.6	0.35
<i>cis-endo-TS-Si</i>	7.7	24.2	2.4	34.3	-52.2	-17.9	12.1	62.4	0.35
<i>cis-exo-TS2-Re</i>	10.9	61.5	3.6	76.0	-81.5	-5.5	22.0	0.0	0.40
<i>cis-exo-TS2-Si</i>	11.3	58.9	5.2	75.4	-80.8	-5.4	23.4	0.0	0.40

^a τ : Occupied probability based on Boltzmann distribution. $\tau = N_i^*/N = [\sum \exp(-\epsilon_i/kT)] / [\sum \exp(-\epsilon_i/kT)]$ (T = 298 K), ee = $(\sum \tau_R - \sum \tau_S) - (\sum \tau_R + \sum \tau_S)$.

To further elucidate the origin of the enantioselectivity and the unusual *exo* selectivity, the four competing TSs were investigated by the combination of the structural and the distortion/interaction analyzes. The result of the distortion/interaction energies for the four TSs indicates that the total distortion energies of the TSs mainly arise from the distortion energies of diene fragment, which suffers heavier distortion compared with the dienophile and catalyst fragments during the ring-closure process. With respect to the *endo* TSs, the distortion of the diene fragment at the *exo* TSs is more serious, and therefore the total distortion energies of the *exo* TSs are disfavored by approximately 20~30 kcal mol⁻¹. However, the ring-formation process proceeding through the *exo* pathway favors the electrophilic/nucleophilic interaction between the dienophile and diene-catalyst fragments, as demonstrated by greater GEDT values (0.50 and 0.52 e) at the two *exo* TSs. The interaction energies completely overwhelm the distortion energies in the *exo* TSs, which might account for

the observed *exo* preference in the reaction. For the two *exo* TSs, the zinc Lewis acid center adopts a tetra-coordination. When the attack of the diene-catalyst complex occurs on the *Re* face of the imine moiety in **1a**, the pyrrole carbon atom is weakly interacted to the zinc center in TS *trans-exo-TS2-Re*, in which the Zn-C bond distance is 2.518 Å. This loose bonding mode places the imine moiety in the empty pocket of the catalyst and then can avoid less steric repulsion from the naphthalene ring of the BINOL ligand. In contrast, the pyrrole nitrogen atom in *trans-exo-TS2-Si* is strongly coordinated to the zinc center with a Zn-N bond distance of 2.355 Å, which forces the dienophile moiety to orientate toward the bulky pocket of the BINOL-Zn catalyst, here it suffers larger steric repulsion from one naphthalene ring of the BINOL ligand. This repulsion is also reflected by distortion energy of the dienophile fragment (12.1 kcal mol⁻¹ in TS *trans-exo-TS2-Re* and 15.6 kcal mol⁻¹ in TS *trans-exo-TS2-Si*). As a result, TS *trans-exo-TS2-Si* is destabilized relative to *trans-exo-TS2-Re* by

3.1 kcal mol⁻¹ in free energy, leading to the preference for the *R* configuration product.

Furthermore, the cycloaddition of **1a** with diene *cis*-**2a** under the chiral catalytic system was investigated to explore the influence of the configuration of diene on the stereochemistry of this reaction. Calculations show that the mechanisms are similar to those obtained in the achiral ZnCl₂-catalyzed reaction system, in which the *cis*-*endo* channel proceeds through a one-step concerted mechanism, whereas the *cis*-*exo* channel undergoes a stepwise mechanism (see PES in Figure S20~21). The difference of these two channels lies in the coordination mode at the zinc center (Figure 7). When the cycloaddition of **1a** with the diene-catalyst complex takes place via the *endo* approach, the carbon atom of the phenyl moiety in **1a** is bonded with the zinc center of the catalyst, leading to formation of a stable tetra-coordination zinc center. However, either the nitrogen atom of the pyrrole moiety or

the carbon atom of the phenyl moiety cannot interact with zinc center when the *exo* approach occurs. Hence, the *exo* TSs are approximately 10.0 kcal mol⁻¹ destabilized in comparison to the *endo* ones, and could not contribute to the product distribution. For the energy-favored *endo* TSs, it is clear that the dienophile moieties are located in the empty pocket of the BINOL ligand, regardless of whether the attack of the diene-catalyst complex originates on the *Re* or *Si* face of imine moiety. The dienophile moieties suffer less steric hindrance from the naphthalene ring of the BINOL ligand, as indicated by similar distortion energies that deformed from the two *endo* TSs (Table 3). Thus, the energy difference between the two competing TSs is only 0.3 kcal mol⁻¹, suggesting that no preference for producing the (*R*)-**3a** and (*S*)-**3a** in kinetics. That is to say, the BINOL ligand cannot allow efficient chiral induction for **1a** when the ester C=O group of diene adopts the *cis* configuration.

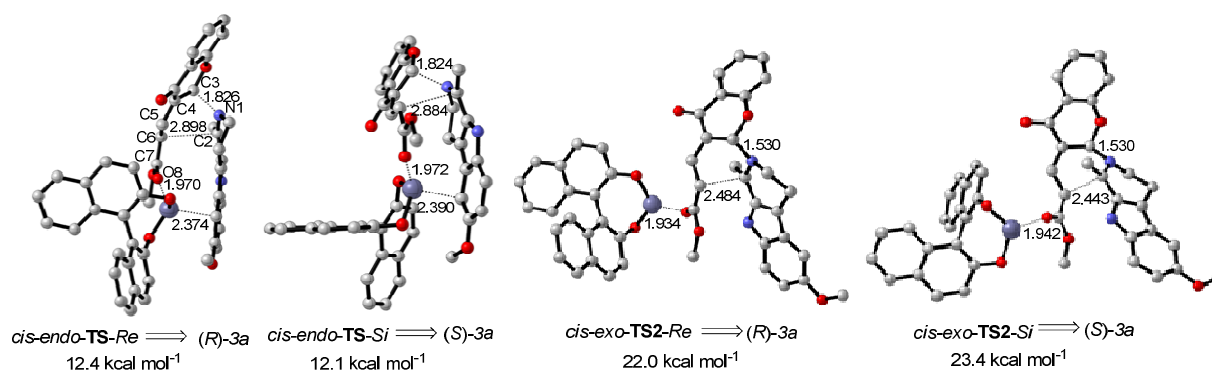


Figure 7. M05-2X/6-31G(d)-optimized ring-closure transition states in the IEDIDA reaction between **1a** and *cis*-**2a** catalyzed by the chiral BINOL-Zn complex (the forming bond distances are labeled in Å and the relative free energies are given in kcal mol⁻¹, respectively).

Overall, it can be predicted that the stereochemistry of the IEDIDA reaction is controlled by a combination of electrophilic/nucleophilic interaction between **1a** and diene-catalyst complex, the configuration of the diene and the asymmetric induction from the BINOL ligand. The cycloaddition via the *exo* approach favors GEDT from the nucleophilic **1a** to the electrophilic, even though the two fragments suffer large distortion. The ester C=O group of diene **2a** with the *trans* configuration permits the formation of a stabilizing interaction between the zinc center of the chiral catalyst and the dienophile moiety, leading to the generation of an energy-favored four-coordinated TS. As a result, the steric hindrance from the naphthalene ring of the BINOL ligand can effectively shields the *Si* face of the imine moiety in **1a**, making the attack of the *Re* face of the imine moiety more accessible.

Conclusions

The reaction mechanism and stereochemistry of the IEDIDA reaction between the cyclic imine **1a** and the electron-poor chromone diene **2a** catalyzed by chiral BINOL-zinc complex has

been theoretically investigated by a combination of DFT calculations, chemical reactivity indices and distortion/interaction analyses. The major conclusions are listed below:

1. The cycloaddition of imine **1a** with diene-ZnCl₂ complex that formed by the coordination of Lewis acid zinc to the ester C=O group of the diene **2a** is the most energy-preferable channel for the generation of [4+2] cycloadduct. The computed activation energy is much lower than that in the uncatalyzed reaction as well as the catalytic model hypothesized in the original experimental paper.¹¹
2. The Lewis acid zinc catalyst plays an important role in increasing the electrophilicity of diene and changes the mechanism from a concerted to a stepwise one because a large stabilization of the corresponding zwitterionic intermediate via the charge delocalization.
3. The catalytic reaction mechanism as well as the stereochemistry of the cycloadduct is sensitive to the configuration of the diene. When the ester C=O group adopts *trans* configuration relative to the C=C double bond, a stabilizing interaction between zinc center of the catalyst and the phenyl moiety of the dienophile can be formed, which

favors the steric discrimination by the BINOL ligand. The imine suffers less repulsion from the naphthalene ring of the BINOL ligand, when the electrophilic attack of diene-catalyst complex takes place from its *Re* face.

4. The *exo*-selectivity is predicted for the cycloadduct, which is attributed to the favorable electrophilic/nucleophilic interaction between the imine and diene-catalyst complex.

Acknowledgements

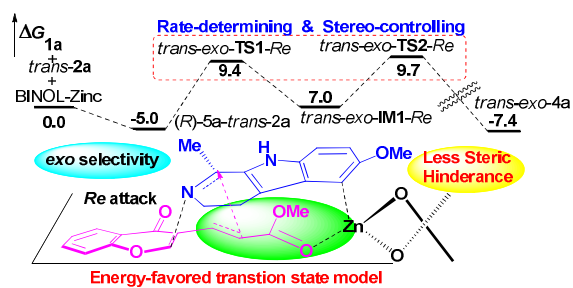
The authors are grateful for the financial support from the National Natural Science Foundation of China (Nos. 21402158), the Scientific Research Fund of Education Department of Sichuan Province (Nos. 14ZB0131), Key Scientific Research Found of Xihua University (Nos. Z1313319) and Open Research Subject of Key Laboratory (Research center for advanced computation) of Xihua University (Nos. szjj2015-051).

Notes and references

- (a) H. Waldmann, *Synthesis*, 1994, 535; (b) G. R. Heintzelman, I. R. Y. Meigh, R. Mahajan, and S. M. Weinreb, *Org. React.*, 2005, **65**, 141; (c) G. Masson, C. Lalli, M. Benohoud, and G. Dagousset, *Chem. Soc. Rev.*, 2013, **42**, 902; (d) V. V. Kouznetsov, *Tetrahedron*, 2009, **65**, 2721; (e) G. B. Rowland, E. B. Rowland, Q. Zhang, and J. C. Antilla, *Curr. Org. Chem.*, 2006, **10**, 981; (f) P. R. Girling, T. Kiyob, and A. Whiting, *Org. Biomol. Chem.*, 2011, **9**, 3105; (g) Y. Kumar, P. Singh, G. Bhargava, *Synlett*, 2015, **26**, 363.
- (a) P. M. Weintraub, J. S. Sabol, J. M. Kane, and D. R. Borcherding, *Tetrahedron*, 2003, **59**, 2953; (b) M. G. P. Buffat, *Tetrahedron*, 2004, **60**, 1701; (c) F.-X. Felpin, and J. Lebreton, *Curr. Org. Synth.*, 2004, **1**, 83; (d) M. Bazin, C. Kuhn, *J. Comb. Chem.*, 2005, **7**, 302; (e) A. R. Katritzky, S. Rachwal, and B. Rachwal, *Tetrahedron*, 1996, **52**, 15031; (f) V. Sridharan, P. A. Suryavanshi, and J. C. Menéndez, *Chem. Rev.*, 2011, **111**, 7157.
- (a) S. Kobayashi, S. Komiyama, and H. Ishitani, *Angew. Chem., Int. Ed.*, 1998, **37**, 3121; (b) S. Kobayashi, K.-I. Kusakabe, Komiyama, and H. Ishitani, *J. Org. Chem.*, 1999, **64**, 4220; (c) S. Kobayashi, K.-I. Kusakabe, and H. Ishitani, *Org. Lett.*, 2000, **2**, 1225; (d) S. Kobayashi, M. Ueno, S. Saito, Y. Mizuki, H. Ishitani, and Y. Yamashita, *Proc. Natl. Acad. Sci. U. S. A.*, 2004, **101**, 5476; (e) Y. Yamashita, Y. Mizuki, and S. Kobayashi, *Tetrahedron Lett.*, 2005, **46**, 1803; (f) V. Jurčík, K. Arai, M. M. Salter, Y. Yamashita, and S. Kobayashi, *Adv. Synth. Catal.*, 2008, **350**, 647; (g) S. Kobayashi, K. Arai, H. Shimizu, Y. Ihori, H. Ishitani, and Y. Yamashita, *Angew. Chem., Int. Ed.*, 2005, **44**, 761; (h) K. Arai, M. M. Salter, Y. Yamashita, and S. Kobayashi, *Angew. Chem., Int. Ed.*, 2007, **46**, 955; (i) K. Arai, S. Lucarini, M. M. Salter, K. Ohta, Y. Yamashita, and S. Kobayashi, *J. Am. Chem. Soc.*, 2007, **129**, 8103; (j) S. Guillarme, and A. Whiting, *Synlett*, 2004, 711; (k) L. Di Bari, S. Guillarme, J. Hanan, A. P. Henderson, J. A. K. Howard, G. Pescitelli, M. R. Probert, P. Salvadori, and A. Whiting, *Eur. J. Org. Chem.*, 2007, 5771.
- (a) S. Yao, M. Jøhannsen, R. G. Hazell, and K. A. Jørgensen, *Angew. Chem., Int. Ed.*, 1998, **37**, 3121; (b) S. Yao, S. Saaby, R. G. Hazell, and K. A. Jørgensen, *Chem.–Eur. J.*, 2000, **6**, 2435; (c) N. S. Josephsohn, M. L. Snapper, and A. H. Hoveyda, *J. Am. Chem. Soc.*, 2003, **125**, 4018; (d) C. A. Newman, J. Antilla, C. P. Chen, A. V. Predeus, L. Fielding, W. D. Wulff, *J. Am. Chem. Soc.*, 2007, **129**, 7216; (e) X. Liu, L. Lin, and X. Feng, *Acc. Chem. Res.*, 2011, **44**, 574; (f) D. J. Shang, J. Y. Xin, L. Liu, X. Zhou, X. Liu, and X. Feng, *J. Org. Chem.*, 2008, **73**, 630; (g) Z. Chen, L. Lin, D. Chen, J. Li, X. Liu, and X. Feng, *Tetrahedron Lett.*, 2010, **51**, 3088; (h) Y. L. Liu, D. J. Shang, X. Zhou, X. Liu, and X. Feng, *Chem. Eur. J.*, 2009, **15**, 2055; (i) Y. L. Liu, D. J. Shang, X. Zhou, Y. Zhu, L. Lin, X. Liu, and X. Feng, *Org. Lett.*, 2010, **12**, 180.
- (a) T. Itoh, M. Yokoya, K. Miyauchi, K. Nagata, and A. Ohsawa, *Org. Lett.* 2003, **5**, 4301; (b) T. Itoh, M. Yokoya, K. Miyauchi, K. Nagata, and A. Ohsawa, *Org. Lett.* 2006, **8**, 1533.
- (a) T. Akiyama, Y. Tamura, J. Itoh, K. Fuchibe, *Synlett*, 2006, 141; (b) J. Itoh, K. Fuchibe, T. Akiyama, *Angew. Chem., Int. Ed.*, 2006, **45**, 4796.
- M. Rueping, and C. Azap, *Angew. Chem., Int. Ed.*, 2006, **45**, 7832.
- (a) J. Esquivias, R. Gómez Arrayás, and J. C. Carretero, *J. Am. Chem. Soc.*, 2007, **129**, 1480; (b) J. Esquivias, I. Alonso, R. Gómez Arrayás, and J. C. Carretero, *Synthesis*, 2009, 113.
- (a) M. He, J. R. Struble, and J. W. Bode, *J. Am. Chem. Soc.*, 2006, **128**, 8418; (b) T.-Y. Jian, P.-L. Shao, and S. Ye, *Chem. Commun.* 2011, **47**, 2381; (c) S. Dong, X. Liu, X. Chen, F. Mei, Y. Zhang, B. Gao, L. Lin, and X. Feng, *J. Am. Chem. Soc.*, 2010, **132**, 10650.
- (a) P. Buonora, J. C. Olsen, T. Oh, *Tetrahedron*, 2001, **57**, 6099; (b) X. X. Jiang, and R. Wang, *Chem. Rev.*, 2013, **113**, 5515.
- V. Eschenbrenner-Lux, P. Küchler, S. Ziegler, K. Kumar, and H. Waldmann, *Angew. Chem., Int. Ed.*, 2014, **53**, 2134.
- (a) Y. Zhao and D. G. Truhlar, *Theor. Chem. Acc.*, 2008, **120**, 215; (b) Y. Zhao and D. G. Truhlar, *Acc. Chem. Res.*, 2008, **41**, 157; (c) M. D. Wodrich, C. Corminboeuf, P. R. Schreiner, A. A. Fokin, and P. von R. Schleyer, *Org. Lett.*, 2007, **9**, 1851.
- (a) E. A. Amin, and D. G. Truhlar, *J. Chem. Theory Comput.*, 2008, **4**, 75; (b) A. Sorkin, D. G. Truhlar, and E. A. Amin, *J. Chem. Theory Comput.*, 2009, **5**, 1254; (c) L. Schiaffino, G. Ercolani, *Chem. Eur. J.* 2010, **16**, 3147; (d) W. Li, Z. Su, C. Hu, *Chem. Eur. J.* 2013, **19**, 124.
- (a) R. Ditchfield, W. J. Hehre and J. A. Pople, *J. Chem. Phys.*, 1971, **54**, 724; (b) W. J. Hehre, R. Ditchfield and J. A. Pople, *J. Chem. Phys.*, 1972, **56**, 2257; (c) P. C. Hariharan and J. A. Pople, *Mol. Phys.*, 1974, **27**, 209; (d) M. S. Gordon, *Chem. Phys. Lett.*, 1980, **76**, 163; (e) P. C. Hariharan and J. A. Pople, *Theor. Chem. Acc.*, 1973, **28**, 213; (f) J. P. Blaudeau, M. P. McGrath, L. A. Curtiss and L. Radom, *J. Chem. Phys.*, 1997, **107**, 5016; (g) M. M. Francl, W. J. Pietro, W. J. Hehre, J. S. Binkley, M. S. Gordon, D. J. DeFrees and J. A. Pople, *J. Chem. Phys.*, 1982, **77**, 3654; (h) R. C. Binning, Jr and L. A. Curtiss, *J. Comput. Chem.*, 1990, **11**, 1206; (i) V. A. Rassolov, J. A. Pople, M. A. Ratner and T. L. Windus, *J. Chem. Phys.*, 1998, **109**, 1223; (j) V. A. Rassolov, M. A. Ratner, J. A. Pople, P. C. Redfern and L. A. Curtiss, *J. Comput. Chem.*, 2001, **22**, 976.
- (a) C. Gonzalez, and H. B. Schlegel, *J. Chem. Phys.*, 1989, **90**, 2154; (b) C. Gonzalez, and H. B. Schlegel, *J. Phys. Chem.*, 1990, **94**, 5523.
- A. V. Marenich, C. J. Cramer, and D. G. Truhlar, *J. Phys. Chem. B* 2009, **113**, 6378.
- (a) L. R. Domingo, *Tetrahedron*, 2002, **58**, 3765; (b) L. R. Domingo, M. J. Aurell, P. Pérez and R. Contreras, *Tetrahedron*, 2002, **58**, 4417; (c) L. R. Domingo, A. Asensio and P. Arroyo, *J. Phys. Org. Chem.* 2002, **15**, 660; (d) L. R. Domingo and J. Andrés, *J. Org. Chem.*, 2003, **68**, 8662; (e) L. R. Domingo, E. Chamorro and P. Pérez, *J. Org. Chem.*, 2008, **73**, 4615; (f) L. R. Domingo and J. A. Sáez, *Org. Biomol. Chem.*, 2009, **7**, 3576;
- (a) R. G. Parr, L. von Szentpály and S. Liu, *J. Am. Chem. Soc.*, 1999, **121**, 1922; (b) Y. Yamaguchi, Y. Osamura and H. F. Schaefer, *J. Am. Chem. Soc.*, 1983, **105**, 7512.
- The global electrophilicity index ω , which measures the stabilization energy when the system acquires an additional electronic charge ΔN from the environment, is given in terms

- of the electronic chemical potential μ and chemical hardness η by the following simple expression: $\omega[\text{eV}] = (\mu^2/2\eta)$. Both quantities can be calculated in terms of the HOMO and LUMO electron energies, ϵ_{H} and ϵ_{L} , as $\mu \approx (\epsilon_{\text{H}} + \epsilon_{\text{L}})/2$ and $\eta \approx (\epsilon_{\text{H}} - \epsilon_{\text{L}})$, respectively. The nucleophilicity index N_{TS} based on the HOMO energies obtained within the Kohn–Sham scheme, is defined as $N = E_{\text{HOMO(Nu)}} - E_{\text{HOMO(TCE)}}$. The nucleophilicity is taken relative to tetracyanoethylene (TCE) as a reference, because it has the lowest HOMO energy in a large series of molecules already investigated in the context of polar cycloadditions.
- 20 L. R. Domingo, M. J. Aurell, P. Pérez, and J. A. Sáez, *RSC ADV.*, 2013, **3**, 1486.
- 21 L. R. Domingo. *RSC ADV.*, 2014, **3**, 32415.
- 22 (a) A. E. Reed, and F. Weinhold, *J. Chem. Phys.* 1985, **83**, 1736; (b) A. E. Reed, R. B. Weinstock, and F. Weinhold, *J. Chem. Phys.* 1985, **83**, 735; (c) A. E. Reed, L. A. Curtiss, and F. Weinhold, *Chem. Rev.* 1988, **88**, 899; (d) A. E. Reed, and P. R. Schleyer, *J. Am. Chem. Soc.*, 1990, **112**, 1434.
- 23 (a) G. Zhong, B. Chan, and L. Radom, *THEOCHEM*, 2007, **811**, 13; (b) D. H. Ess, and K. N. Houk, *J. Am. Chem. Soc.*, 2007, **129**, 10646; (c) C. Gordon, J. L. Mackey, J. C. Jewett, E. M. Sletter, K. N. Houk, and C. R. Bertozzi, *J. Am. Chem. Soc.*, 2012, **134**, 9199; (d) D. H. Ess, G. O. Jones, and K. N. Houk, *Org. Lett.*, 2008, **10**, 1633; (e) F. Liu, R. S. Paton, S. Kim, Y. Liang, K. N. Houk, *J. Am. Chem. Soc.* 2013, **135**, 15642; (f) H. V. Pham, R. S. Paton, A. G. Ross, S. J. Danishefsky, and K. N. Houk, *J. Am. Chem. Soc.*, 2014, **135**, 2397.
- 24 M. J. Frisch, et al. *Gaussian 09, Revision A.02*; Gaussian, Inc., Wallingford CT, 2009.
- 25 C. Y. Legault, CYLview, 1.0b, Université de Sherbrooke, Sherbrooke, Québec, Canada, 2009, <http://www.cylview.org>.
- 26 P. Jaramilio, and L. R. Domingo, E. Chamorro, and P. Pérez, *THEOCHEM*, 2008, **865**, 68.
- 27 (a) M. Roberson, A. S. Jepsen, and K. A. Jørgensen, *Tetrahedron* 2001, **57**, 90; (b) L. R. Domingo, M. Oliva, and J. Andrés, *J. Org. Chem.*, 2001, **66**, 6157. (c) A. Bongini, and M. Panunzio, *Eur. J. Org. Chem.* 2006, 972. (d) Z. Pi, S. Li, *J. Phys. Chem. A* 2006, **110**, 9225; (e) N. Çelebi-Ölçüm, D. H. Ess, V. Aviyente, K. N. Houk, *J. Org. Chem.* 2008, **73**, 7472; (e) Z. Su, S. Qin, C. Hu, and X. Feng, *Chem. Eur. J.* 2010, **16**, 4359.
- 28 (a) G. Ujaque, P. S. Lee, K. N. Houk, M. F. Hentemann, and S. J. Danishefsky, *Chem. Eur. J.* 2002, **8**, 3423; (b) H. Audrian, J. Thorhauge, R. G. Hazell, and K. A. Jørgensen, *J. Org. Chem.* 2000, **65**, 4487; (c) S. Danishefsky, E. Larson, D. Askin, and N. Kato, *J. Am. Chem. Soc.*, 1985, **107**, 1246; (d) D. H. Ess, G. O. Jones, and K. N. Houk, *Adv. Synth. Catal.*, 2006, **348**, 2337; (e) S. A. Cinar, S. Ercan, S. E. Gunal, I. Dogan, V. Aviyente, *Org. Biomol. Chem.*, 2014, **12**, 8079; (f) P. Rooshenas, K. Hof, P. R. Schreiner, and C. M. Williams, *Eur. J. Org. Chem.* 2011, 983; (g) N. Nikbin, P. T. Do, S. Caratzoulas, R. F. Lobo, P. Dauenhauer, D. G. Vlachos, *J. Catal.* 2013, **297**, 35. (h) Z. Su, and C. K. Kim, *Org. Biomol. Chem.*, 2015, **13**, 6313.

Graphic Abstract.



The enantioselectivity is originated from the hindrance of BINOL ligand, and the exo-selectivity is achieved by the favored electrophilic/nucleophilic interaction.